Chapter 15

TRANSITION AND SPACE-CHARGE MISMATCH

The slippage factor has been defined as

$$\eta = \frac{1}{\gamma_t^2} - \frac{1}{\gamma^2} \ , \tag{15.1}$$

where $E = \gamma E_0$ is the total energy of the synchronous particle having rest energy E_0, and $\gamma_t E_0$ is the transition energy of the lattice. As the particle crosses transition through ramping, the slippage factor passes through zero and switches sign from negative to positive. The synchrotron angular frequency is defined as

$$\omega_s = \sqrt{-\frac{eh\eta V_{\rm rf} \cos\phi_s}{2\pi\beta^2 E}}\ \omega_0 \ , \tag{15.2}$$

where $V_{\rm rf}$ is the rf voltage, h the rf harmonic, ϕ_s the synchronous phase, β the velocity of the synchronous particle with respect to the velocity of light, and ω_0 the revolution angular frequency. Because of its dependency on η, the synchrotron frequency also slows down as transition is approached. Thus, the motion of the particle cannot follow the rf bucket in the longitudinal phase space. Here, we first study the kinematics as the bunch is ramped through transition, and then the space-charge mismatch of the bunch lengths below and above transition.

15.1 EQUATIONS OF MOTION

Physically, η measures the amount of time or phase slippage of a bunch particle with respect to the synchronous particle. Thus, for a particle with energy deviation ΔE, its rf phase $\Delta\phi$ slips at a rate of

$$\frac{d\Delta\phi}{dt} = \frac{h\eta\,\omega_0}{\beta^2 E}\Delta E \ . \tag{15.3}$$

At the same time, this off-energy particle receives additional energy from the rf cavities at the rate of

$$\frac{d\Delta E}{dt} = \frac{eV_{\rm rf}\omega_0}{2\pi}\left[\sin(\phi_s+\Delta\phi) - \sin\phi_s\right] \ . \tag{15.4}$$

Formerly, when we characterize the beam particle by τ, its arrival time ahead of the synchronous particle, the right side of $d\tau/ds$ in Eq. (3.8) or (3.10) is preceded by a negative sign, implying that for a positive momentum offset, the particle will arrive late ($\tau < 0$) above transition ($\eta > 0$). Here, $\Delta\phi$ is the slip in rf phase relative to the synchronous particle. When the particle arrives late at the cavity gap, the rf phase will have evolved more than $2\pi h$. Thus, the rf phase slip is positive and so is the sign preceding the right side of Eq. (15.3). Eliminating ΔE, we obtain for small $\Delta\phi$ the equation governing the motion of the phase of the particle:

$$\frac{d}{dt}\left(\frac{\beta^2 E}{h\eta\omega_0}\frac{d\Delta\phi}{dt}\right) - \frac{eV_{\rm rf}\cos\phi_s\omega_0}{2\pi}\Delta\phi = 0 \ . \tag{15.5}$$

Unlike our previous discussion, β, E, η, and ω_0 vary with time and should not be taken out from the first derivative operator. This is especially true for η which appears in the denominator. However, as an approximation, we can neglect the slow time variations of all the parameters except η/E. This leads to

$$\frac{d}{dt}\left(\frac{E}{\eta}\frac{d\Delta\phi}{dt}\right) - \left(\frac{heV_{\rm rf}\cos\phi_s\omega_0^2}{2\pi\beta^2}\right)\Delta\phi = 0 \ . \tag{15.6}$$

Under the approximation that the second bracketed term is considered time independent and also the variation of η/E is linear in time near transition,* or

$$\frac{\eta}{E} = \frac{2\dot\gamma_t\, t}{\gamma_t^4 E_0} \ , \tag{15.7}$$

Eq. (15.6) can be solved exactly in terms of Bessel functions of fractional orders [3]. However, all the important features of the solution can be estimated easily without going

*Some authors assume η to be linear in t instead. In that case, one needs also the additional assumption that $\dot\gamma_t T_c \ll 1$.

into the differential equation and Bessel functions [1]. Best of all, through the estimation, one can have a clear picture of what is going on during transition. In Eq. (15.7), the time t is measured from transition. Thus, $t < 0$ is below transition and $t > 0$ is above. On the other hand, the subscript t implies evaluation of the respective quantity at the moment when transition is crossed. Thus,

$$\dot{\gamma}_t = \frac{eV_{\rm rf}\omega_0}{2\pi E_0} \sin\phi_s \tag{15.8}$$

is the rate at which γ is ramped right at transition.

We can also rewrite Eq. (15.6) in the form

$$\frac{d}{dt}\left(\frac{1}{\omega_s^2}\frac{d\Delta\phi}{dt}\right) + \Delta\phi = 0 \ , \tag{15.9}$$

where ω_s is given by Eq. (15.2). However, Eq. (15.2) should be considered as a definition of ω_s only. This is because the beam particle does not follow the invariant trajectory of the Hamiltonian when it is near transition and therefore does not make synchrotron oscillations, so that ω_s, as defined by Eq. (15.2), loses its meaning of frequency.

15.2 NON-ADIABATIC TIME

When η^{-1} is not rapidly changing, a bucket can be defined. The bucket height is given by

$$(\Delta E)_{\rm bucket} \propto \left(\frac{E}{|\eta|}\right)^{1/2} \ . \tag{15.10}$$

However, as the bunch particle passes through transition, η^{-1} changes rapidly. Here, we follow the assumption of a linear time variation for η/E as given by Eq. (15.7), while all other parameters such as the rf voltage and the synchronous phase, aside from flipping from ϕ_s to $\pi - \phi_s$, are held fixed near transition. This means that when transition is approached, synchrotron frequency is slowed down to zero and the bucket height is increased to infinity. In other words, when it is close enough to transition, the particle will not be able to catch up with the rapid changing of the bucket shape. This time period, from $t = -T_c$ to $t = T_c$ is called the non-adiabatic region, and T_c the *non-adiabatic time*. Here, we define this region by

$$\omega_s \leq \frac{2}{(\Delta E)_{\rm bucket}} \frac{d(\Delta E)_{\rm bucket}}{dt} \ . \tag{15.11}$$

The right side is

$$\frac{2}{(\Delta E)_{\rm bucket}}\frac{d(\Delta E)_{\rm bucket}}{dt}\bigg|_{t=-T_c} = 2\,\frac{d}{dt}\sqrt{\frac{T_c}{-t}} = \sqrt{\frac{T_c}{(-t)^3}} = \frac{1}{T_c}\ . \tag{15.12}$$

Evaluating at $t=-T_c$, the left side of Eq. (15.11) is

$$\omega_s|_{t=-T_c} = \sqrt{\frac{h\dot{\gamma}_t T_c e V_{\rm rf}\cos\phi_s}{\pi\gamma_t^4 E_0}}\,\omega_\infty\ , \tag{15.13}$$

where $\omega_\infty = \omega_0/\beta$ and is time independent. We then obtain the non-adiabatic time from Eq. (15.11):

$$T_c = \left[\left(\frac{\beta_t\gamma_t^4}{2\omega_\infty h}\right)\left(\frac{|\tan\phi_s|}{\dot{\gamma}_t^2}\right)\right]^{1/3}\ , \tag{15.14}$$

where the expression of $\dot{\gamma}_t$ in Eq. (15.8) has been used. Note that the non-adiabatic time is just an approximate time. The factor 2 on the right side of Eq. (15.11) was inserted for the purpose that T_c given by Eq. (15.14) is exactly the same as the adiabatic time quoted in the literature. We have written Eq. (15.14) in such a way that the factor in the first brackets contains parameters of the lattice, while $\dot{\gamma}_t$ in the second brackets is determined by the ramp curve and ϕ_s, the synchronous phase at transition, is determined by the rf-voltage table.

15.3 BUNCH SHAPE AT TRANSITION

For the sake of simplicity, we adopt a model which states that,
(1) when $|t| > T_c$, the beam particles follow the bucket with synchrotron oscillations, and
(2) when $|t| < T_c$, the beam particles make no synchrotron oscillations at all.

At $t=-T_c$, the beam particle still follows the bucket. Therefore, From Eq. (15.3), the bunch length σ_ϕ is related to the rms energy spread $\sigma_{_E}$ by

$$\nu_s\sigma_\phi = \frac{h|\eta|}{\beta_t^2\gamma_t E_0}\,\sigma_{_E}\ , \tag{15.15}$$

where η is to be evaluated at $t=-T_c$, and the energy E is evaluated approximately right at transition since the change is slow. The 95% bunch area is defined as

$$S = 6\pi\sigma_\tau\sigma_{_E}\ , \tag{15.16}$$

where this expression should hold in the adiabatic region. From Eqs. (15.15) and (15.16), we obtain the rms bunch length in time $\sigma_\phi = h\omega_0\sigma_\tau$ as

$$\sigma_\tau = \left(\frac{S|\eta|}{6\pi\nu_s\omega_0\beta_t^2\gamma_t E_0}\right)^{1/2} . \tag{15.17}$$

Substituting $\eta(-T_c)$ from Eq. (15.7) and $\omega_s(-T_c)$ from Eqs. (15.11) and (15.12), we arrive at

$$\sigma_\tau = \frac{1}{\sqrt{3\pi}}\left(\frac{ST_c^2\dot{\gamma}_t}{\beta_t^2\gamma_t^4 E_0}\right)^{1/2} . \tag{15.18}$$

Our simple model requires no synchrotron oscillation inside the non-adiabatic region. This is equivalent to having $\eta = 0$ in Eq. (15.3); or the phase of each particle will not change at all. Therefore, Eq. (15.18) is also the bunch length right at transition, where the exact expression from solving the differential equation is

$$\sigma_\tau = \frac{2}{3^{5/6}\Gamma(\frac{1}{3})}\left(\frac{ST_c^2\dot{\gamma}_t}{\beta_t^2\gamma_t^4 E_0}\right)^{1/2} . \tag{15.19}$$

This just amounts to the replacement of $1/\sqrt{3\pi} = 0.326$ by $2/[3^{5/6}\Gamma(\frac{1}{3})] = 0.300$, where $\Gamma(\frac{1}{3}) = 2.678939$ is the Gamma function. Our estimate is about 8.8% too large because our simple model does not allow the bunch to continue to shrink in the non-adiabatic region.

On the other hand, without synchrotron oscillations, the energy of each beam particle is accelerated by the focusing rf force according to Eq. (15.4). From $t = -T_c$ to $t = 0$, a particle at a phase offset $\Delta\phi$ from the synchronous particle will acquire an energy

$$\Delta E = T_c E_0 \frac{d\dot{\gamma}}{d\Delta\phi}\Delta\phi , \tag{15.20}$$

where, according to Eq. (15.4),

$$\frac{d\dot{\gamma}}{d\Delta\phi} \approx \frac{\dot{\gamma}_t}{\tan\phi_s} , \tag{15.21}$$

and the small phase-offset approximation has been made. At $t = -T_c$, when there are still synchrotron oscillations in our simple model, if we write the phase offset as

$$\Delta\phi = \widehat{\Delta\phi}\cos\omega_s t , \tag{15.22}$$

according to the phase-drift equation, the energy spread of the particle is

$$\Delta E = -\frac{\nu_s\beta_t^2\gamma_t E_0}{h\eta}\widehat{\Delta\phi}\sin\omega_s t = -\frac{\nu_s\beta_t^2\gamma_t E_0}{h\eta}\sqrt{\widehat{\Delta\phi}^{\,2} - (\Delta\phi)^2} , \tag{15.23}$$

where $\widehat{\Delta\phi} = \sqrt{6}\sigma_\tau h\omega_0$ is the half width of the bunch at $t = -T_c$ as given by Eq. (15.18). When evaluated at $t = -T_c$, it is found that the coefficient of Eq. (15.23) is equal to that of Eq. (15.20), and we denote it by

$$a = -\frac{\nu_s \beta_t^2 \gamma_t E_0}{h\eta} = T_c E_0 \frac{d\dot{\gamma}}{d\Delta\phi} \ . \tag{15.24}$$

Therefore, the total energy spread at transition is given by

$$(\Delta E)_{\text{total}} = a\left[\sqrt{\widehat{\Delta\phi}^{\,2} - (\Delta\phi)^2} + \Delta\phi\right] \ . \tag{15.25}$$

The maximum total energy spread comes out to be

$$(\Delta E)_{\text{total, max}} = \frac{1}{\sqrt{\pi}}\left(\frac{S\beta_t^2\gamma_t^4 E_0}{T_c^2\dot{\gamma}_t}\right)^{1/2} \tag{15.26}$$

at $\Delta\phi = 2^{-1/2}\widehat{\Delta\phi}$. The exact value from the solution of a differential equation is

$$(\Delta E)_{\max} = \frac{\Gamma(\frac{1}{3})}{3^{1/6}2^{1/2}\pi}\left(\frac{S\beta_t^2\gamma_t^4 E_0}{T_c^2\dot{\gamma}_t}\right)^{1/2} \ , \tag{15.27}$$

or just a replacement of $1/\sqrt{\pi} = 0.564$ by $\Gamma(\frac{1}{3})/(3^{1/6}2^{1/2}\pi) = 0.502$. By the same token, the particle at the tail of the bunch will be decelerated by the same energy. Particles in between will be accelerated accordingly. The bunch shape at transition is therefore given by Fig. 1, which is slanted at an angle from the ΔE-axis. Our estimate of $(\Delta E)_{\text{total}}$ is about 11% too large. This is to be expected because we allow pure increment in energy by the focusing rf potential in the non-adiabatic region without any motion in the phase direction.

As we recall, the maximum energy spread at transition is *not* derived via Eq. (15.16) and one should not expect Eq. (15.16) to hold in the non-adiabatic region. Here, we derive another expression for the bunch area right at transition. Using Eqs. (15.18) and (15.26) and the fact that the maximum half bunch length is $\hat{\tau} = \sqrt{6}\sigma_\tau$, we obtain the bunch area

$$S = \frac{1}{\sqrt{2}}\,\pi\hat{\tau}\widehat{\Delta E} \tag{15.28}$$

If the exact solutions in Eqs. (15.19) and (15.30) are used, one gets instead

$$S = \frac{\sqrt{3}}{2}\,\pi\hat{\tau}\widehat{\Delta E} \ , \tag{15.29}$$

or the replacement of $1/\sqrt{2} = 0.707$ by $\sqrt{3}/2 = 0.866$. Notice that so far we are still within a Hamiltonian system so that the bunch area should be conserved. The fact that the bunch area is now less than $\pi\hat{\tau}\widehat{\Delta E}$ indicating that the bunch ellipse has been tilted, as illustrated in Fig. 15.1. This is because phase motion in the non-adiabatic region has almost (totally in our simplified model) been frozen and the energy change has been uneven along the bunch. This problem will be studied again in the next section.

To conclude this section, let us write the rms time spread and rms energy spread at transition as well as the non-adiabatic time in terms of the parameters that we can control, namely, the synchronous phase ϕ_s and ramping rate $\dot{\gamma}_t$ (Exercise 15.1):

$$\sigma_\tau \propto \frac{\tan^{\frac{1}{3}}\phi_s}{\dot{\gamma}_t^{\frac{1}{6}}}\ , \qquad \sigma_E \propto \frac{\dot{\gamma}_t^{\frac{1}{6}}}{\tan^{\frac{1}{3}}\phi_s}\ , \qquad T_c \propto \frac{\tan^{\frac{1}{3}}\phi_s}{\dot{\gamma}_t^{\frac{2}{3}}}\ . \tag{15.30}$$

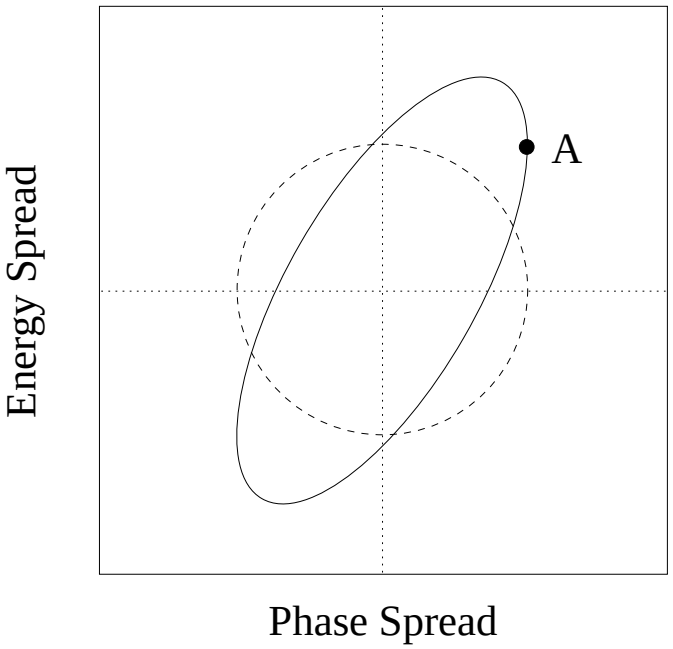

Figure 15.1: The evolution of the bunch, according to the simple model, from $t = -T_c$ (dashes) to the time when transition is crossed (solid). In the exact solution of the differential equation, there is an additional shrinkage in the phase spread of the ellipse. Point A indicates that when the phase offset is at a maximum, the energy offset is not at a maximum.

15.4 MORE SOPHISTICATED APPROXIMATION

15.4.1 ADIABATIC REGION

We now discard the simple model in the previous section and come back to Eq. (15.9), the equation governing motion of small phase offset. Instead of solving the differential equation exactly, we are looking into approximates instead. In the adiabatic region that is not too far away from transition, the particle is performing synchrotron oscillations with a slowly changing frequency $\omega_s/2\pi$ given by Eq. (15.2). The solution of Eq. (15.9) is therefore of the form

$$\Delta\phi = Ae^{i\int \omega_s dt} \ , \tag{15.31}$$

where the amplitude A is also slowly changing with time. We then have

$$\frac{d}{dt}\left(\frac{1}{\omega_s^2}\frac{d\Delta\phi}{dt}\right) = -\Delta\phi + \left[\left(\frac{2i\dot{A}}{\omega_s} - \frac{iA\dot{\omega}_s}{\omega_s^2}\right) + \left(\frac{\ddot{A}}{\omega_s^2} - \frac{2\dot{A}\dot{\omega}_s}{\omega^3}\right)\right] e^{i\int \omega_s dt} \ . \tag{15.32}$$

Since $\Delta\phi$ varies much faster than A and ω_s, we can neglect $\ddot{A}$, $\ddot{\omega}_s$, and $\dot{A}\dot{\omega}_s$, and set

$$\frac{2\dot{A}}{\omega_s} = \frac{A\dot{\omega}_s}{\omega_s^2} \ , \tag{15.33}$$

so that Eq. (15.9) is satisfied. The relation in Eq. (15.33) leads to

$$\frac{A^2}{\omega_s} = \text{ constant} \ , \tag{15.34}$$

implying that the solution of Eq. (15.9) or the rf phase of a beam particle in the adiabatic region can be written as

$$\Delta\phi = B\sqrt{\omega_s}\, e^{i\int \omega_s dt} \ , \tag{15.35}$$

with B being constant.

The dropping of the slowly varying terms from Eq. (15.32) is equivalent to assuming

$$\frac{\ddot{A}}{\omega_s^2} \ll \frac{A\dot{\omega}_s}{\omega_s^2} \ , \tag{15.36}$$

$$\frac{2\dot{A}\dot{\omega}_s}{\omega_s^3} \ll \frac{A\dot{\omega}_s}{\omega_s^2} \ . \tag{15.37}$$

Again, with the assumption of constant rf voltage $V_{\rm rf}$, constant synchronous phase ϕ_s, and linear time variation of η/E, we can write, using Eqs. (15.2), (15.7), and (15.8),

$$\omega_s^2(t) = b|t| \qquad \text{with} \qquad b = \frac{\dot{\gamma}_t he V_{\rm rf} |\cos\phi_s| \omega_\infty^2}{\pi \gamma_t^4 E_0} \ . \tag{15.38}$$

Then, together with Eq. (15.34), it is easy to show that (Exercise 15.2),

$$\text{Eq. (4.6)} \quad \Longrightarrow \quad |t| \gg \left(\frac{3}{8}\right)^{2/3} \left(\frac{1}{b}\right)^{1/3} \ , \tag{15.39}$$

$$\text{Eq. (4.7)} \quad \Longrightarrow \quad |t| \gg \left(\frac{1}{2}\right)^{2/3} \left(\frac{1}{b}\right)^{1/3} \ . \tag{15.40}$$

In other words, the adiabatic solution is only valid if Eqs. (15.39) and (15.40) hold. A non-adiabatic time T_c can therefore be defined by letting

$$T_c = \left(\frac{1}{b}\right)^{1/3} \ , \tag{15.41}$$

which turns out to be exactly the same expression as our former definition in Eq. (15.12). Here, we arrive at a neat way to remember the non-adiabatic time:

$$\omega_s^2 = \frac{|t|}{T_c^3} \qquad \text{or} \qquad \omega_s\big|_{t=-T_c} = \frac{1}{T_c} \ . \tag{15.42}$$

Now, let us continue the study of the bunch shape in the adiabatic region. Differentiating Eq. (15.35) and using Eq. (15.34), we get

$$\frac{d\Delta\phi}{dt} = iB\omega_s^{3/2} \left[1 - \frac{i}{4}\left(\frac{T_c}{|t|}\right)^{3/2}\right] e^{i\int \omega_s dt} \ , \tag{15.43}$$

or

$$\frac{d\Delta\phi}{dt} = i\omega_s \Delta\phi \left[1 + \frac{1}{16}\left(\frac{T_c}{|t|}\right)^{3}\right]^{1/2} e^{-i\varphi} \ , \tag{15.44}$$

with

$$\varphi = \tan^{-1} \frac{1}{4}\left(\frac{T_c}{|t|}\right)^{3/2} \ . \tag{15.45}$$

Then, using Eq. (15.3), we arrive at the energy offset of the particle

$$\Delta E = i\omega_s \Delta\phi \frac{\beta^2\gamma E_0}{|\eta| h\omega_0} \left[1 + \frac{1}{16}\left(\frac{T_c}{|t|}\right)^{3}\right]^{1/2} e^{-i\varphi} \ . \tag{15.46}$$

We see from Eq. (15.35) that, as the bunch is approaching the non-adiabatic region, its width shrinks in the same way as the decrease of $\sqrt{\omega_s}$. On the other hand, from Eq. (15.46), the height of the bunch increases because of the square root term and the $t^{-1/4}$ dependency in the front factor. We also see that there is a phase advance φ of the energy offset, or a tilt in the bunch shape in the longitudinal phase space. This tells us that there is already slowing down in the phase motion in the adiabatic region when transition is approached. This reminds us again that there is no clear cut boundary between the adiabatic and non-adiabatic regions.

The next task is to relate the constant B to the bunch area. The motion of the particle described by Eqs. (15.35) and (15.46) is of the form

$$\Delta\phi = \widehat{\Delta\phi}\cos\theta \ , \qquad \Delta E = \widehat{\Delta E}\sin(\varphi-\theta) \ , \tag{15.47}$$

which map out a tilted ellipse of area

$$S = \pi\frac{\widehat{\Delta\phi}}{h\omega_0}\widehat{\Delta E}\cos\varphi \ , \tag{15.48}$$

inscribed inside the rectangle of half-width $\widehat{\Delta\phi}/(h\omega_0)$ and half-height $\widehat{\Delta E}$, and this is the bunch area in eV-s.

The half bunch length in the adiabatic region can be read off from Eq. (15.35):

$$\widehat{\Delta\phi} = B\omega_s^{1/2} \ . \tag{15.49}$$

Substituting into Eq. (15.46), we obtain the half energy spread

$$\widehat{\Delta E} = \frac{\beta^2\gamma E_0}{|\eta|h\omega_0}\,\omega_s^{3/2}\left[1+\frac{1}{16}\left(\frac{T_c}{|t|}\right)^3\right]^{1/2} \ . \tag{15.50}$$

where the last square bracket term is just $\sec\varphi$, as given by Eq. (15.45). When they are substituted in the bunch area in Eq. (15.48), the constant B will be determined,

$$S = \frac{B^2 eV_{\rm rf}|\cos\phi_s|}{2h} \ , \tag{15.51}$$

which is time independent as anticipated.

Using the linear time dependency of ω_s^2 from Eq. (15.42) and replacing the constant B with Eq. (15.51), we obtain the time dependency of the half bunch length,

$$\widehat{\Delta\phi} = \left(\frac{2hS}{eV_{\rm rf}|\cos\phi_s|T_c}\right)^{1/2}\left(\frac{|t|}{T_c}\right)^{1/4} \ , \tag{15.52}$$

and also

$$\widehat{\Delta E} = \frac{\omega_0}{\pi}\left(\frac{hSeV_{\rm rf}|\cos\phi_s|T_c}{2}\right)^{1/2}\left(\frac{T_c}{|t|}\right)^{1/4}\left[1+\frac{1}{16}\left(\frac{T_c}{|t|}\right)^3\right]^{1/2} . \tag{15.53}$$

Through the definition of the non-adiabatic time, the half bunch length and half energy spread can be written in the form that resembles the expressions in Eqs. (15.19) and (15.27):

$$\widehat{\Delta\phi} = h\omega_0\left(\frac{2ST_c^2\dot{\gamma}_t}{\pi\beta_t^2\gamma_t^4E_0}\right)^{1/2}\left(\frac{|t|}{T_c}\right)^{1/4} , \tag{15.54}$$

and also the

$$\widehat{\Delta E} = \left(\frac{S\beta_t^2\gamma_t^4E_0}{2\pi T_c^2\dot{\gamma}_t}\right)^{1/2}\left(\frac{T_c}{|t|}\right)^{1/4}\left[1+\frac{1}{16}\left(\frac{T_c}{|t|}\right)^3\right]^{1/2} . \tag{15.55}$$

15.4.2 NON-ADIABATIC REGION

We can also study the non-adiabatic region of the Eq. (15.14), which can be transformed to

$$\frac{d}{dx}\left(\frac{1}{|x|}\frac{d\Delta\phi}{dx}\right)+\Delta\phi = 0 , \tag{15.56}$$

where $x = t/T_c$ and use has been made of Eq. (15.38). However, we find it easier to solve instead the differential equation governing energy offset, which reads

$$\frac{d^2\Delta E}{dx^2}+|x|\Delta E = 0 . \tag{15.57}$$

We would like to introduce a *normalized* energy-offset

$$\Delta p(x) = \frac{2\pi}{\omega_0 eV_{\rm rf}\cos\phi_s T_c}\,\Delta E(x) = \frac{\tan\phi_s}{\dot{\gamma}_t E_0 T_c}\,\Delta E(x) . \tag{15.58}$$

so that $\Delta p(x)$ will have the same dimension as $\Delta\phi$, the energy equation of motion becomes the simple relation

$$\Delta\phi = -\,\mathrm{sgn}(x)\frac{d\Delta p}{dx} . \tag{15.59}$$

For the sake of convenience, we concentrate on the situation above transition only where $x \geq 0$ so that the absolute-value sign can be dropped and $\mathrm{sgn}(x)$ can be ignored. At the end, we can replace x by $|x|$ everywhere in the solution so that it applies to both above and below transition. Note that both $\cos\phi_s$ and $\tan\phi_s$ are now negative.

To seek for a solution within the non-adiabatic region where $|x| < 1$, it is natural to resort to power series:

$$\Delta p = \sum_{n=0}^{\infty} a_n x^{n+k} \ , \tag{15.60}$$

where k is to be determined. Substitution into of Eq. (15.57) leads to

$$\sum_{n=-3}^{\infty} a_{n+3}(n+k+3)(n+k+2)x^{n+k+1} + \sum_{n=0}^{\infty} a_n x^{n+k+1} = 0 \ . \tag{15.61}$$

The indicial equations determine that $k = 0$ and $a_2 = 0$. The solution can be written as

$$\Delta p = \Big(a_0 + a_3 x^3 + a_6 x^6 + \cdots\Big) + \Big(a_1 x + a_4 x^4 + a_7 x^7 + \cdots\Big) \ , \tag{15.62}$$

where the coefficients are related by the recurrence relation

$$a_{n+3} = -\frac{a_n}{(n+3)(n+2)} \ . \tag{15.63}$$

Thus, there are two free constants a_0 and a_1, which are to be expected from a second-order differential equation. It is more convenient to rewrite Eq. (15.62) as

$$\Delta p = a_0\Big(1 + a_3' x^3 + a_6' x^6 + \cdots\Big) + a_1\Big(x + a_4' x^4 + a_7' x^7 + \cdots\Big) \ , \tag{15.64}$$

where we have redefined the coefficients as $a_n' = a_n/a_0$ for $n = 3, 6, 9, \cdots$, and $a_n' = a_n/a_1$ for $n = 4, 7, 8, \cdots$. They can be readily computed from the recurrence relation:

$$\begin{cases} a_3' = -\dfrac{1}{(3.2)} \ , \ a_6' = +\dfrac{1}{(6.5)(3.2)} \ , \ a_9' = -\dfrac{1}{(9.8)(6.5)(3.2)} \ , \ \cdots \ , \\ a_4' = -\dfrac{1}{(4.3)} \ , \ a_7' = +\dfrac{1}{(7.6)(4.3)} \ , \ a_{10}' = -\dfrac{1}{(10.9)(7.6)(4.3)} \ , \ \cdots \ , \end{cases} \tag{15.65}$$

where the periods or dots in above denote multiplication. The phase offset can now be obtained using Eq. (15.59):

$$\Delta\phi = -a_0\Big(3a_3' x^2 + 6a_6' x^5 + \cdots\Big) - a_1\Big(1 + 4a_4' x^3 + 7a_7' x^6 + \cdots\Big) \ . \tag{15.66}$$

Now we are going to derive the trajectory of a particle which is at its maximum phase offset right at transition. Thus we obtain

$$-a_1 = \widehat{\Delta\phi}_0 = \frac{2^{3/2} h\omega_0}{3^{1/3}\Gamma(\frac{1}{3})}\left(\frac{ST_c^2\dot{\gamma}_t}{\beta_t^2\gamma_t^4 E_0}\right)^{1/2} \ , \tag{15.67}$$

with the aid of Eq. (15.19), where an extra subscript "0" has been added to denote "right at transition" or $x = 0$ for the sake of clarity. This position of the beam particle corresponds to Point A in Fig. 15.1, where the energy offset is *not* at its maximum, but is related to it by

$$\Delta E = \widehat{\Delta E}_0 \sin\varphi \ , \tag{15.68}$$

where φ is the tilde angle referenced in Eq. (15.47), and it modifies the expression of bunch area to $S = \pi\widehat{\tau}_0\widehat{\Delta E}_0 \cos\varphi$. However, from Eq. (15.29), the angle is found to be $\cos\varphi = \sqrt{3}/2$. We therefore have

$$a_0 = \frac{1}{2}\,\widehat{\Delta p}_0 = \frac{1}{2}\,\frac{|\tan\phi_s|}{\dot{\gamma}_t E_0 T_c}\,\widehat{\Delta E}_0 = \frac{1}{2}\,\frac{3^{1/6}\Gamma^2(\frac{1}{3})}{2\pi}\,\widehat{\Delta\phi}_0 \ , \tag{15.69}$$

where Eqs. (15.19) and (15.27) have been used, and obtain the relation

$$\frac{a_1}{a_0} = -\frac{2\widehat{\Delta\phi}_0}{\widehat{\Delta p}_0} = \frac{4\pi}{3^{1/6}\Gamma^2(\frac{1}{3})} \ . \tag{15.70}$$

Thus the trajectory of the beam particle is governed by

$$\Delta p(x) = \widehat{\Delta\phi}_0 \left[-x\left(1 + a_4' x^3 + a_7' x^6 + \cdots\right) - \frac{a_0}{a_1}\left(1 + a_3' x^3 + a_6' x^6 + \cdots\right)\right] \ , \tag{15.71}$$

$$\Delta\phi(x) = \widehat{\Delta\phi}_0 \left[\left(1 + 4a_4' x^3 + 7a_7' x^6 + \cdots\right) + \frac{a_0}{a_1}\left(3a_3' x^2 + 6a_6' x^5 + 9a_9' x^8 + \cdots\right)\right] \ . \tag{15.72}$$

However, we are not so interested in the motion of a single particle. What we wish to derive are the half width and half energy spread of a bunch at different times. For this, we have to solve an envelope equation given by Eq. (15.89) below with the space-charge coefficient $n_{\rm spch}$ set to zero. However, that is a nonlinear equation which is difficult to tackle. Instead, we try to extract the bunch length energy from the solution we obtained in Eqs. (15.71) and (15.72). To accomplish this, we introduce an ensemble of beam particles at the phase ellipse. This can be easily done by writing out the general solution of the differential equation [Eq. (15.57)] by a taking a linear combination of the Eq. (15.71) or (15.72) and another solution of the differential equation. Thus, we have

$$\begin{aligned}\Delta p(x) = \ \widehat{\Delta\phi}_0 \Bigg\{ &\cos\psi \left[-x\Big(1 + a_4' x^3 + a_7' x^6 + \cdots\Big) - \frac{a_0}{a_1}\Big(1 + a_3' x^3 + a_6' x^6 + \cdots\Big)\right] \\ &- \sin\psi \left[\frac{\sqrt{3}a_0}{a_1}\Big(1 + a_3' x^3 + a_6' x^6 + \cdots\Big)\right]\Bigg\} \ ,\end{aligned} \tag{15.73}$$

$$\Delta\phi(x) = \widehat{\Delta\phi}_0 \Bigg\{ \cos\psi \left[\Big(1 + 4a_4' x^3 + 7a_7' x^6 + \cdots\Big) + \frac{a_0}{a_1}\Big(3a_3' x^2 + 6a_6' x^5 + 9a_9' x^8 + \cdots\Big) \right] + \sin\psi \left[\frac{\sqrt{3}a_0}{a_1}\Big(3a_3' x^2 + 6a_6' x^5 + 9a_9' x^8 + \cdots\Big) \right] \Bigg\} , \tag{15.74}$$

where $-\sqrt{3}a_0/a_1$ is included purely for convenience and the relation $\Delta\phi = -d\Delta p/dx$ still holds. One constant in these equation is $\widehat{\Delta\phi}_0$, the maximum phase offset of the phase ellipse at $x = 0$. In fact, it solely determines bunch area or the area of the ellipse (Exercise 15.4). The other constant is the phase angle ψ, which represents different particles on the ellipse in the longitudinal phase space.

As a first application, at $x = 0$, Eq. (15.73) becomes

$$\Delta p(x) = -\widehat{\Delta\phi}_0 \frac{a_0}{a_1}\Big(\cos\psi + \sqrt{3}\sin\psi\Big) , \tag{15.75}$$

whose maximum occurs when $\psi = \pi/3$. This gives the normalized energy spread at transition

$$\widehat{\Delta p}_0 = -\frac{2a_0}{a_1}\,\widehat{\Delta\phi}_0 , \tag{15.76}$$

agreeing with what we have in Eq. (15.70). The phase spread at transition is trivial because only the cosine term in Eq. (15.74) contributes.

Now let us proceed up to the order x. The energy spread in Eq. (15.73) gives

$$\Delta p(x) = -\widehat{\Delta\phi}_0 \frac{a_0}{a_1}\left[\cos\psi\left(1 + \frac{a_1}{a_0}\,x\right) + \sqrt{3}\sin\psi\right] . \tag{15.77}$$

For the maximum,

$$\cos\psi = \frac{1}{2}\left(1 + \frac{3a_1}{4a_0}\,x\right) \quad \text{and} \quad \sin\psi = \frac{\sqrt{3}}{2}\left(1 - \frac{a_1}{4a_0}\,x\right) . \tag{15.78}$$

Thus, the half energy spread is

$$\widehat{\Delta p}(x) = \widehat{\Delta p}_0\left[1 + \frac{a_1}{4a_0}\,x\right] = \widehat{\Delta p}_0\left[1 - \frac{\pi}{3^{1/6}\Gamma^2\left(\frac{1}{3}\right)}\,x\right] . \tag{15.79}$$

There is no $\mathcal{O}(x)$ in the correction to the half bunch length. The next order is $\mathcal{O}(x^2)$:

$$\Delta\phi(x) = \widehat{\Delta\phi}_0 \left[\cos\psi \left(1 - \frac{a_0}{2a_1}\, x^2 \right) - \sin\psi\, \frac{\sqrt{3}a_0}{2a_1}\, x^2 \right] , \tag{15.80}$$

whose maximum occurs when $\psi = \mathcal{O}(x^2)$. Thus the half bunch length becomes

$$\widehat{\Delta\phi}(x) = \widehat{\Delta\phi}_0 \left[1 - \frac{a_0}{2a_1}\, x^2 \right] = \widehat{\Delta p}_0 \left[1 + \frac{3^{1/6}\Gamma^2\left(\frac{1}{3}\right)}{8\pi}\, x^2 \right] . \tag{15.81}$$

Higher orders in x of the half energy spread and half bunch length of the bunch can therefore be computed.

It is evident that from time $|t|$ in the non-adiabatic region to the time when transition is crossed, the shrinkage of the bunch length is of order $(|t|/T_c)^2$ and is therefore small, while the increase in energy spread is of order $(|t|/T_c)$ which is much larger. This explains why in the simple model of Sec. 15.3, we can just approximate the bunch length at transition to be the bunch length at the non-adiabatic time. On the other hand, we have to compute the increase in energy spread within the non-adiabatic region more accurately.

There is an important comment on why that particular combination of independent solutions are used for the phase ellipse in Eq. (15.73) or (15.74). We choose the trajectory in Eqs. (15.71) and (15.72) as one of the independent solution so as to ensure that at the time when transition is crossed the bunch ellipse will be tilted to the correct amount, so that the half bunch length and half energy spread will be correct. Any other combination is also a valid solution of the differential equation, but it will lead to the bunch ellipse to be tilted differently at transition, which in turn implies the possible unphysical situation that the bunch does not fit the rf bucket when it is well below transition.

In passing, we list the exact solution for the phase offset and energy offset:

$$\begin{aligned} \Delta p(x) &= A\, y^{1/3} \left[\cos\psi_1 J_{-1/3}(y) + \sin\psi_1 N_{-1/3}(y) \right] , \\ \left(\tfrac{2}{3}\right)^{1/3} \Delta\phi(x) &= A\, y^{2/3} \left[\cos\psi_1 J_{2/3}(y) + \sin\psi_1 N_{2/3}(y) \right] , \end{aligned} \tag{15.82}$$

where $y = \frac{2}{3}|x|^{3/2}$, and J and N are the Bessel and Neumann functions or order $\frac{2}{3}$ or $-\frac{1}{3}$. Here, A and ψ_1 are the two constants. Unlike our solution, this solution is valid for all x. When we are very far from transition, or $|x| \gg 1$, the Bessel functions have the

asymptotic expansions:

$$\begin{aligned} J_\nu(y) &\approx \sqrt{\frac{2}{\pi y}} \cos\left[y - \frac{\pi}{2}\left(\nu + \frac{1}{2}\right)\right] \ , \\ N_\nu(y) &\approx \sqrt{\frac{2}{\pi y}} \sin\left[y - \frac{\pi}{2}\left(\nu + \frac{1}{2}\right)\right] \ . \end{aligned} \tag{15.83}$$

Thus, Δp and $\Delta\phi$ are 90° out of phase, or the bunch fits the bucket far from transition. Therefore, at the moment when transition is crossed, the bunch ellipse will be tilted to the right amount so that one can read off the correct half bunch length and the half energy spread. This explains why we have chosen the combination of $J_{-1/3}$ and $N_{-1/3}$ for Δp in Eq. (15.82) instead of, for example, $J_{-1/3}$ and $J_{1/3}$. This method of asymptotic behavior cannot be applied to the power-series solution we pursuit in this section, because the power-series solution is only valid when $|x| < 1$.

15.5 SPACE-CHARGE MISMATCH

In the previous section, the equations of motion are symmetric about the transition time. This means that the bunch becomes shorter and taller while approaching transition, but restores its shape after crossing transition. Most important of all, the equilibrium bunch length is continuous across transition and the bunch area remains constant. However, the introduction of space-charge will break this symmetry. Below transition, the space-charge force is repulsive. The rf potential well is distorted, resulting in the lengthening of the bunch. But the situation is different above transition. With the switching of sign of the slippage factor, the space-charge force changes sign also. Now it becomes attractive. It adds constructively to the rf focusing force and the equilibrium bunch length becomes shorter instead. This is illustrated in the top plot of Fig. 15.2.

A space-charge parameter can easily be defined. We have derived in Eq. (4.18) the reactive force on a beam particle due to a reactive impedance, which is proportional to the gradient of the longitudinal beam profile. If we assume a parabolic beam profile, this reactive force is linear. Thus, for a linearized rf voltage, the space-charge force implies the replacement,

$$\Big[eV_{\rm rf}\cos\phi_s\Big]\Delta\phi \longrightarrow \Big[eV_{\rm rf}\cos\phi_s\Big]\Delta\phi - \frac{3\pi N_b r_p E_0 g_0 h^2}{R\gamma_t^2 \widehat{\Delta\phi}^3}\,\Delta\phi \ , \tag{15.84}$$

where N_b is the number of particles per bunch with half width $\widehat{\Delta\phi}$ in rf radian, r_p the classical particle radius, and R the accelerator radius. Use has been made of the fact that

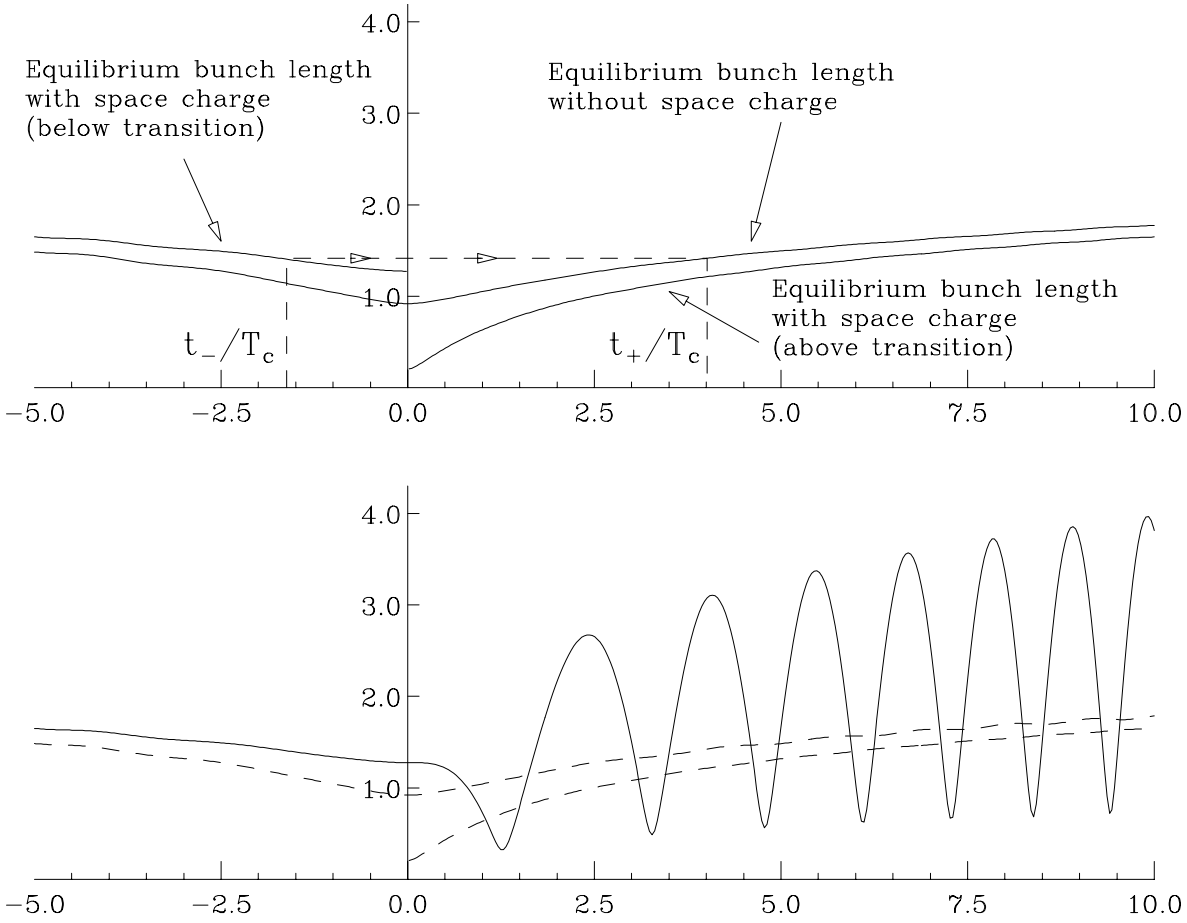

Figure 15.2: Bunch length is plotted versus x, time normalized to the non-adiabatic time T_c, across transition. Below transition (negative time), the space-charge force is repulsive, thus giving a longer equilibrium bunch length. Above transition (positive time), the space-charge force becomes attractive and therefore shortens the equilibrium bunch length. Top plot shows the mismatch of equilibrium bunch length across transition. A possible transition jump from $x = t_-/T_c$ to $x = t_+/T_c$ should have bunch length matched from the beginning to the end of jump, and is therefore asymmetric with respect to $x = 0$. Lower plot shows the bunch that matches to the space-charge distorted bucket below transition overshoots after crossing transition and oscillates about the shorter equilibrium length.

the reactive impedance is the space-charge impedance $Z_0^{\parallel}/n = iZ_0 g_0/(2\beta_t\gamma_t^2)$ at transition energy as given by Eq. (4.14). Notice that $\cos\phi_s$ changes sign from positive to negative on crossing transition. Thus, the space-charge force counteracts the rf force below transition and enhances the rf force above. The ratio of the space-charge force to the rf force is

$$\eta_{\rm spch} = \frac{3\pi N_b r_p E_0 g_0 h^2}{R\gamma_t^2 e V_{\rm rf} |\cos\phi_s| \widehat{\Delta\phi}^3} \ . \tag{15.85}$$

This ratio is, however, time dependent, because the bunch length changes with time. One can evaluate this ratio right at transition and called it the *space-charge parameter*. Thus

$$\eta_{\rm spch}(0) = \frac{9\Gamma^3(\frac{1}{3})}{16\sqrt{2}} \frac{N_b r_p g_0 h}{R} \left[\frac{\beta_t E_0}{Sh\omega_0}\right]^{3/2} \left[\frac{h\omega_0}{\beta_t\dot{\gamma}_t}\right]^{1/2} \ , \tag{15.86}$$

where use has been made of Eq. (15.19). Figure 15.2 is computed according to the space-charge parameter $\eta_{\rm spch}(0) = 2$.

Thus, as soon as transition is crossed, the bunch will find itself not able to fit the rf bucket. The bunch tumbles inside the bucket performing synchrotron oscillations in the quadrupole mode. In the worst situation, there will be beam loss. Even if the bucket is large enough to hold the bunch, the bunch area will increase due to filamentation. Such phenomenon has been observed in the Fermilab Booster, Main Ring, and the present Main Injector. A longitudinal quadrupole damping has been installed in each of the rings to cope with the oscillations. Such a damper consists mainly of a pickup which sends signals to modify the rf voltage, which in turn damp the oscillations. Figure 15.3 shows such a mismatched oscillation at the Fermilab Main Ring. In the top plot, the quadrupole damper is turned off. The lowest trace, which is green in color, measures the bunch length by comparing the spectral signal of the third rf harmonic to the fundamental. The bunch length goes through a minimum around 0.78 s when transition is crossed. After that it oscillates at twice the synchrotron frequency in the quadrupole mode with increasing amplitude, as a result of the space-charge mismatch of the equilibrium bunch lengths before and after transition. Note that the quadrupole synchrotron period is diminishing away from transition due to the fact the slippage factor η is increasing. In the lower plot, the quadrupole damper is turned on. The lowest trace, which is green in color, measures the bunch length. It is evident that although there are some quadrupole oscillations after transition, they are of much smaller amplitudes and are completely damped later.

15.5.1 MATHEMATICAL FORMULATION

Mathematically, this phenomenon can be formulated as follows. As a result of

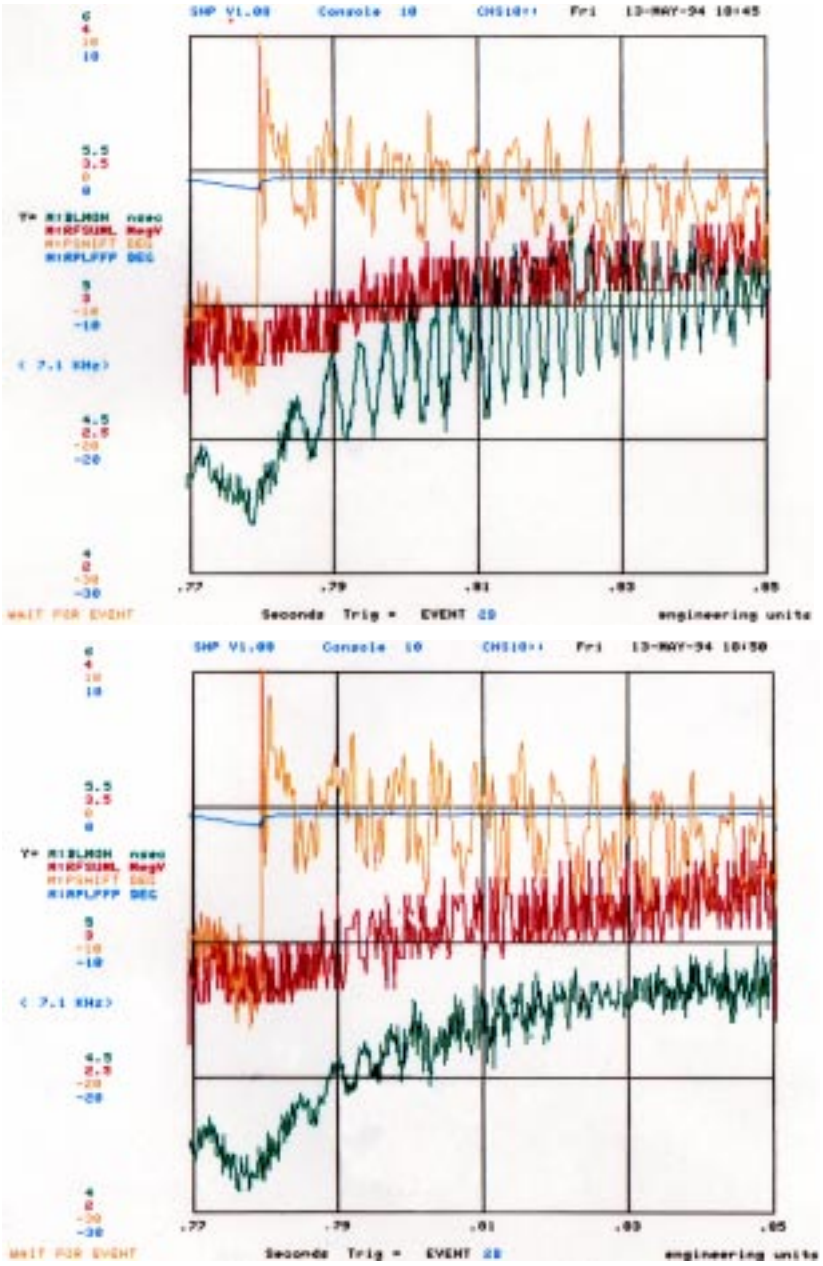

Figure 15.3: (color) A bunch is crossing transition at the Fermilab Main Ring. The lowest (green) trace of the top plot measures the bunch length. It dips to a minimum at $\sim$ 0.78 s when transition is crossed. It then oscillates at twice the synchrotron frequency with large amplitudes due to space-charge mismatch. In the lower plot, the quadrupole damper is turned on. Quadrupole oscillations of small amplitudes are seen in the lowest (green) trace after transition and are completely damped later.

Eqs. (15.84) and (15.86), the equation of motion governing $\Delta\phi$ is modified from Eq. (15.9) to

$$\frac{d}{dt}\left[\frac{1}{\omega_s^2}\frac{d\Delta\phi}{dt}\right] + \Delta\phi + \mathrm{sgn}(t)\frac{n_{\mathrm{spch}}}{\widehat{\Delta\phi}^3}\,\Delta\phi = 0 \ , \tag{15.87}$$

where $n_{\mathrm{spch}} = \eta_{\mathrm{spch}}\widehat{\Delta\phi}^3$ and is no more time dependent. In terms of the normalized time coordinate $x = t/T_c$, the differential equation becomes

$$\frac{d}{dx}\left[\frac{1}{x}\frac{d\Delta\phi}{dx}\right] + \mathrm{sgn}(x)\Delta\phi + \frac{n_{\mathrm{spch}}}{\widehat{\Delta\phi}^3}\,\Delta\phi = 0 \ . \tag{15.88}$$

The half bunch length $\widehat{\Delta\phi}$, however, satisfies a slightly different differential equation,

$$\frac{d}{dx}\left[\frac{1}{x}\frac{d\widehat{\Delta\phi}}{dx}\right] + \mathrm{sgn}(x)\widehat{\Delta\phi} + \frac{n_{\mathrm{spch}}}{\widehat{\Delta\phi}^2} - x\,\frac{(S_N/\pi)^2}{\widehat{\Delta\phi}^3} = 0 \ , \tag{15.89}$$

where S_N is a *normalized dimensionless* bunch area when the bunch ellipse is transformed to a circle. It is related to our usual bunch area in eV-s by

$$S_N = \frac{2h^2\omega_0^2\dot{\gamma}_t T_c^2}{\beta_t^2\gamma_t^4 E_0}\,S \ . \tag{15.90}$$

The derivation was first given by Sørenssen [3]. It is rather involved and is omitted here. However, this is the same as the single-particle equation except for the extra last term. Such an extra last term also arises in the Kapchinskij-Vladimirskij beam envelope equation for transverse oscillation [4]. In fact, it occurs also in the equation satisfied by the betatron function, where the betatron function takes the place of $\widehat{\Delta\phi}$ while the transverse emittance takes the place of $(S_N/\pi)^2$. This equation cannot be solved analytically. However, when it is far away from transition, $|x| \gg 1$, the variation of $\widehat{\Delta\phi}$ with respect to x should be small, and we obtain the algebraic equation

$$\widehat{\Delta\phi}^4 + \mathrm{sgn}(x)n_{\mathrm{spch}}\widehat{\Delta\phi} = \frac{S_N^2}{\pi^2}\,|x| \ . \tag{15.91}$$

In the absence of space charge, $n_{\mathrm{spch}} = 0$, we recover the solution in Eq. (15.54), namely,

$$\widehat{\Delta\phi} = \left[\frac{S_N}{\pi}\right]^{1/2}|x|^{1/4} = h\omega_0\left[\frac{2ST_c^2\dot{\gamma}_t}{\pi\beta_t^2\gamma_t^4 E_0}\right]^{1/2}|x|^{1/4} \ . \tag{15.92}$$

If we wish, we may also consider this as a derivation of the half-bunch-length differential equation [Eq. (15.89)], since we have already derived this expression for half bunch length and we know that such a term proportional to $\left(\widehat{\Delta\phi}\right)^{-3}$ must exist in an envelope equation.

Equation (15.91), the quartic in bunch length, can be further simplified to

$$\theta^4 + \mathrm{sgn}(x)\eta_{N0}\theta = |x| \ , \tag{15.93}$$

where the *normalized* bunch length θ is defined as

$$\widehat{\Delta\phi} = \sqrt{\frac{S_N}{\pi}}\,\theta = h\omega_0\sqrt{\frac{2\dot{\gamma}_t T_c^2 S}{\pi\beta_t\gamma_t^4 E_0}}\,\theta = \sqrt{\frac{2h\omega_0\dot{\gamma}_t T_c^2 S_c}{\pi\beta_t^2\gamma_t^4}}\,\theta \ , \tag{15.94}$$

and the normalized space-charge parameter is

$$\eta_{N0} = n_{\mathrm{spch}}\left[\frac{\pi}{S_N}\right]^{3/2} = \frac{3\pi^2 N_b r_p g_0 h}{2R}\left[\frac{\beta_t E_0}{S h\omega_0}\right]^{3/2}\left[\frac{h\omega_0}{2\pi\beta_t\dot{\gamma}_t}\right]^{1/2} = \frac{3\pi^2 N_b r_p g_0 h}{2RS_c^{3/2}}\left[\frac{h\omega_0}{2\pi\beta_t\dot{\gamma}_t}\right]^{1/2} , \tag{15.95}$$

where the explicit expression of T_c has been used. In above, S_c is another commonly used dimensionless bunch area, which is defined as

$$S_c = \pi\widehat{\Delta(\beta\gamma)}\widehat{\Delta\phi} = \frac{h\omega_0}{\beta E_0}\,S \ . \tag{15.96}$$

Written in terms of these normalized quantities, the differential equation satisfied by the bunch length is also simplified and becomes

$$\frac{d}{dx}\left[\frac{1}{x}\frac{d\theta}{dx}\right] + \mathrm{sgn}(x)\theta + \frac{\eta_{N0}}{\theta^2} - \frac{x}{\theta^3} = 0 \ . \tag{15.97}$$

Notice that $\widehat{\Delta\phi}/\theta$ is proportional to the bunch length at transition,

$$\widehat{\Delta\phi}_0 = \frac{2^{3/2}h\omega_0}{3^{1/3}\Gamma(\frac{1}{3})}\left[\frac{ST_c^2\dot{\gamma}_t}{\beta_t^2\gamma_t^4 E_0}\right]^{1/2} \ . \tag{15.98}$$

Thus, aside from a constant, θ can also be considered as normalized to the bunch length at transition. In fact, evaluated at transition without space charge, $\theta = 2\pi^{1/2}3^{-1/3}/\Gamma(\frac{1}{3}) = 0.91748$ radian, as indicated in Fig. 15.2. Comparing the original space-charge parameter $\eta_{\mathrm{spch}}(0)$ in Eq. (15.86) with the normalized space-charge parameter η_{N0}, we find

$$\eta_{N0} = \frac{8\pi^{3/2}}{3\left[\Gamma(\frac{1}{3})\right]^3}\,\eta_{\mathrm{spch}}(0) = 0.77233\,\eta_{\mathrm{spch}}(0) \ . \tag{15.99}$$

The lower plot in Fig. 15.2 is derived from solving Eq. (15.97) numerically starting with a bunch that is matched to the equilibrium bunch length far below transition.

We conclude this section by listing in Table 15.1 some transition crossing properties as well as the space-charger parameters of the Fermilab Booster, Fermilab Main Ring, and Fermilab Main Injector. We have used in the table the designed intensity of 6×10^{10} for the Main Injector. At its present commissioned intensity of 4×10^{10}, the space-charge parameter will become $\eta_{\rm spch}(0) = 0.303$ only. Notice that the space-charge parameter for the Fermilab Booster is about ten times those for the Main Ring and Main Injector. Thus, bunch-length oscillations due to space-charge mismatch can be very serious at the Booster before the installation of the quadrupole damper. In fact, this has been one of the reasons of bunch area increases due to filamentation after crossing transition.

Table 15.1: Some transition crossing properties and the space-charge parameters of the Fermilab Booster, Main Ring, and Main Injector.

	Booster	Main Ring	Main Injector	
Circumference	474.203	6283.185	3319.419	m
Transition γ_t	5.373	18.85	21.80	
Revolution frequency f_0	621.157	47.646	90.220	kHz
Rf harmonic h	84	1113	588	
Rf voltage $V_{\rm rf}$	0.763	2.5	2.78	MV
Synchronous angle ϕ_s	53.6	60.0	37.6	degrees
Ramp rate $\dot{\gamma}_t$	406.7	109.94	163.10	s^{-1}
Non-adiabatic time T_c	0.216	3.00	2.14	ms
Number per bunch N_b	3×10^{10}	3×10^{10}	6×10^{10}	
95% bunch area S	0.025	0.15	0.15	eV-s
Rms bunch length at γ_t	0.237	0.335	0.217	ns
Space charge g_0	4.5	4.89	4,34	
$\lvert Z_0^{\parallel}/n\rvert_{\rm spch}$	29.9	2.63	1.72	Ohms
Space-charge parameter $\eta_{\rm spch}(0)$	2.117	0.277	0.455	

15.6 TRANSITION JUMP

A transition jump is a way to go around transition crossing so that all the demise can be avoided [5, 6, 7]. It consists of the following steps. At some time $t = t_- < 0$, the currents of some quadrupoles are triggered so that γ_t of the ring is sudden raised and the

beam becomes far below transition (usually $\Delta\gamma_t \approx -1$). Next, at some time $t = t_+ > 0$, these quadrupoles are triggered back to their original currents and the γ_t of the ring returns to its original value. However, at this moment the beam is far above (usually $\Delta\gamma_t \approx 1$) the original γ_t already. Because we need to avoid the bunch-length mismatch due to space-charge, we need to make sure that the equilibrium bunch lengths at t_- and t_+ are equal. This means that $|t_-| < t_+$, or the transition jump will be asymmetric about $t = 0$. This is illustrated in the top plot of Fig. 15.2 (see also Exercise 15.6).

It is important to understand that a transition jump scheme does not really eliminate the crossing of transition. This is because when the transition gamma is returned to its original value by triggering the quadrupoles the second time, the beam particles that were below transition suddenly find themselves above transition. In other words, transition is crossed by changing suddenly the value of γ_t of the lattice instead of ramping the particles. However, crossing transition this way is much faster than ramping, usually faster by a factor of more than 10. The effective $\dot{\gamma}_t$ is therefore very large and the effective non-adiabatic time becomes very small. The manipulation of the quadrupoles at $t = t_-$ can be much slower because there is no transition crossing during that manipulation. We win here because the demise of crossing transition will not have enough time to develop. On the other hand, changing the lattice of the accelerator ring so fast can bring about other problems also. One possibility is a sudden increase in dispersion resulting in a sudden increase in the horizontal beam size which may lead to beam loss. Recently, Visnijic has been able to limit the propagation of this dispersion wave by the installation of a three-quadrupole cell [8].

15.7 EXERCISES

15.1. Derive the variation of the non-adiabatic time T_c and the rms time and energy spreads of a bunch right at transition with respect to the synchronous phase ϕ_s and the ramping rate $\dot{\gamma}_t$, as given in Eq. (15.30).

15.2. Show that the time evaluation of the phase offset,

$$\Delta\phi(t) = B\sqrt{\omega_s}e^{i\int \omega_s dt} \ , \tag{15.100}$$

where B is a constant, is valid only in the adiabatic region.
Hint: Show that the approximations made in Eqs. (15.36) and (15.37) are in accordance with $t \gg T_c$, where T_c is the non-adiabatic time.

15.3. Show that the half bunch length and half energy spread given by Eqs. (15.52) and (15.53) can also be obtained by relation from the phase equation:

$$\widehat{\Delta\phi} = \frac{h|\eta|\omega_0}{\beta^2 E\omega_s}\widehat{\Delta E} \ , \tag{15.101}$$

together with the assumption of linear time variation of η/E.

15.4. (1) If $f(x)$ and $g(x)$ are two independent solutions of the differential equation (15.57), show that the Wronskian $W(f,g) \equiv f(x)g'(x) - f'(x)g(x)$ is independent of x and can therefore be evaluated at any x, especially at $x = 0$.
(2) The solution can be written as

$$\begin{aligned} \Delta p &= \quad B\left[f(x)\cos\psi + g(x)\sin\psi\right] \ , \\ \Delta\phi &= -B\left[f'(x)\cos\psi + g'(x)\sin\psi\right] \ , \end{aligned} \tag{15.102}$$

where B is a constant. Show that these two equations trace out an ellipse by varying ψ, with the ellipse area $\mathcal{A}$ given by

$$\mathcal{A}^2 \propto (f^2+g^2)(f'^2+g'^2) - (ff'+gg')^2 \ . \tag{15.103}$$

(3) Show that the right side of Eq. (15.103) is equal to the Wronskian $W(f,g)$ and the bunch area is therefore conserved and is determined only by the constant B.

15.5. Show that the power-series expansion of the Eqs. (15.82) gives exactly the same solution as Eqs. (15.73) and (15.74). Note that the ψ in the two solutions can be different.

15.6. A transition jump is to be designed for the Fermilab Main Injector with a total jump of $\Delta\gamma_t = 2.0$. Because of space-charge mismatch of the bunch length near transition, the jump will be asymmetric; i.e., $|t_-| < t_+$, where t_- is the start-jump time before transition and t_+ the end-jump time after transition. Using Eq. (15.93), compute t_-, t_+, $\Delta\gamma_{t-}$, and $\Delta\gamma_{t+}$, where the latter are, respectively, the amounts of jump from $t = t_-$ to $t = 0$ and from $t = 0$ $t = t_+$. For the Main Injector, the ramp rate across transition is $\dot{\gamma}_t = 163.1\ \mathrm{s}^{-1}$ and the non-adiabatic time is $T_c = 2.14$ ms.

Bibliography

[1] K.Y. Ng *Bunch Shape Evolution Near Transition, — an Intuitive Approach*, Fermilab report FN-644, 1996.

[2] I. Kourbanis, private communication; E.C. Raka, *Damping Bunch shape Oscillations in the Brookhaven AGS*, IEEE, **NS16**, 3, 182 (1969).

[3] A. Sørenssen, *The Effect of Strong Longitudinal Space-Charge Forces at Transition,* CERN Report MPS/Int. MU/EP 67-2, 1967.

[4] I.M. Kapchinskij and V.V. Vladimirskij, *Limitations of Proton Beam Current in a strong Focusing Linear Accelerator Associated with the Beam Charge*, International Conference on High Energy Accelerators and Instrumentation, CERN 1959, p.274.

[5] S. Holmes, *Main Injector Transition Jump*, Fermilab Report MI-0008, 1989.

[6] T. Risselada, CERN 4th General Accel. School, Jükuch, Germany, 1990, p.161.

[7] K.Y. Ng and A. Bogacz, *Dispersion γ_t Jump for the Main Injector*, Proceedings of the 1995 Particle Accelerator Conference and International Conference on High Energy Accelerators, Dallas, May 1-5, 1995, p.3340.

[8] V. Visnjic, *Local Dispersion Insert: the γ_t Knob for Accelerators*, Fermilab Report TM-1888, 1994.